Optimal Transmission Radius for Flooding in Large Scale Sensor Networks

Marco Zúñiga Z. and Bhaskar Krishnamachari

Department of Electrical Engineering, University of Southern California,

Los Angeles, CA 90089,USA.

E-mail: {marcozun,bkrishna}@usc.edu

Abstract

One of the principal characteristics of large scale wireless sensor networks is their distributed, multi-hop nature. Due to this characteristic, applications such as query propagation rely regularly on network-wide flooding for information dissemination. If the transmission radius is not set optimally, the flooded packet may be holding the transmission medium for longer periods than are necessary, reducing overall network throughput. We analyze the impact of the transmission radius on the average settling time - the time at which all nodes in the network finish transmitting the flooded packet. Our analytical model takes into account the behavior of the underlying contention-based MAC protocol, as well as edge effects and the size of the network. We show that for large wireless networks there exists an intermediate transmission radius which minimizes the settling time - corresponding to an optimal tradeoff between reception and contention times. We also explain how physical propagation models affect some scenarios and why there is no intermediate optimal transmission radius observed in these cases. The mathematical analysis is supported and validated through extensive simulations.

I. INTRODUCTION

Wireless sensor networks present new challenges due to their unique characteristics, one of them being their distributed, multi-hop, dynamic nature. Due to this characteristic, applications regularly rely on flooding as a robust way to reach all the nodes in the network. Examples of these applications are query propagation in directed diffusion [2] and time distribution in the S-MAC protocol [15].

Despite some well-known drawbacks, flooding is still widely used as a robust technique for information dissemination. However, since flooding depends on the multi-hop distribution of data, factors such as the choice of the transmission radius further influence the efficiency of this task. Adjusting the transmission radius has been studied with intent of finding the optimal radius for different parameters such as network connectivity, but to the best of our knowledge, it has not previously been researched in the context of optimizing flooding events.

It is known that flooding sometimes consumes energy and bandwidth resources unnecessarily. Furthermore, if the transmission radius of the nodes is not carefully chosen, the flooded packet may take too long to be transmitted by all the nodes in the network, impacting overall network throughput: *the more time the channel is captured by a flooding event, the less queries can be disseminated, and the less time the channel is available for other packet transmissions*. We can state the relation between settling time and throughput in sensor networks as follows:

$$throughput \; \alpha \; \frac{1}{settling time} \tag{1}$$

This paper addresses the problem of finding an optimal transmission radius for flooding in sensor networks. The intuitive idea is that there is a general tradeoff in choosing the size of the transmission radius. On one hand, a large transmission radius implies that fewer retransmissions will be needed to reach the outlying nodes in the network; therefore, the message will be heard by all nodes in less time. On the other hand, a larger transmission radius involves a higher number of neighbors competing to access the medium, and therefore each node has a longer

contention delay for packet transmissions. The purpose of our work is the analysis of this tradeoff in CSMA/CA wireless MAC protocols.

Although at first glance this problem appears intuitively simple, our initial results prompted some surprising deviations from our first analytical model [19] that caused us to further analyze the problem in depth. The optimization of the flooding event is heavily dependent on the radio propagation model that is being used, and in light of this we have discovered physical layer characteristics that augment our first analytical model.

The remainder of the paper is organized as follows. Section II positions our work in the literature, discussing other related work. Section III describes an intuitive analytical model that we developed to obtain the optimal transmission radius in sensor networks. Section IV shows the preliminary results obtained through simulations that verify our analytical information. Section V, describes scenarios that deviated from the first analytical model, and physical layer characteristics that explain these deviations. Section VI outlines our conclusions and intents for future work.

II. RELATED WORK

Even though flooding has some unique advantages – it maximizes the probability that all reachable nodes inside a network will receive the packet – it has several disadvantages as well. Several works have proposed mechanisms to improve flooding efficiency. The broadcast storm paper by Ni *et al.* [3] suggests a way to improve flooding by trading robustness. In that work, the authors propose to limit the number of nodes that transmit the flooded packet. The main idea is to have some nodes refrain from forwarding their packet if its transmission will not contribute to a larger coverage. Nevertheless, the basic flooding technique is in wide use for a number of querying techniques for sensor networks (in large part because of its guarantee of maximal robustness), and we focus on analyzing its MAC-layer effects and improving its performance by minimizing the settling time of flooding.

Other studies have looked at the impact of the transmission radius in wireless networks. In [5] and [8] the authors analyzed the critical transmission range to maintain connectivity in wireless networks. [5] presents a statistical

analysis of the probability of connectivity and [8] provides a separate algorithm to accomplish this connectivity. On the same line of work, [6] and [7] analyze the minimum number of neighbors that a node should have to keep the network connected.

In [10], the authors describe a similar tradeoff for increasing the transmission radius: a shorter range implies less collisions and a longer range implies moving a packet further ahead in one hop. However, in that work the authors want to maximize a parameter called *the expected one-hop progress in the desired direction*, which essentially measures how fast a packet can reach its destination in point-to-point transmissions. The same tradeoff is studied in [20], however the goal in this work is to maximize the number of data packets delivered in the network.

Another important direction in the study of optimal transmission radius is targeted to improve network lifetime and energy consumption. In [21], Wattenhofer *et al.* propose a simple distributed algorithm, where each node can vary its transmission radius to increase network lifetime while maintaining connectivity. [22] investigates the effects of transmission radius in the energy efficiency of packet transmission. This study also shows how some parameters of the physical layer model influence the performance of protocols at the network layer.

It is important to remark that all these previous studies were not analyzing a protocol like flooding, but instead trying to obtain an optimal transmission radius for other metrics such as connectivity, throughput or energy. In [4] an experimental testbed of 150 Berkeley motes [9] run flooding as the routing protocol. The study showed empirical relations between the reception and settling times – parameters used in our work – for different transmission ranges.

Our work also finds an optimal transmission radius. However, in our case the important metric is the amount of time that a flooded packet captures the transmission medium. To accomplish the goal of minimizing the settling time, we study the tradeoff between reception and contention times. To our knowledge, there are few other papers in the literature that undertake a detailed analysis of the interaction between the MAC-layer and network-level behavior of an information dissemination scheme in wireless networks.
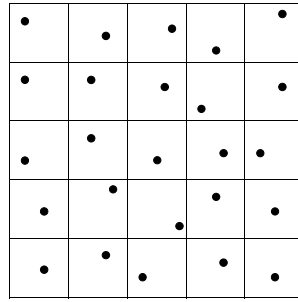
Fig. 1.   Uniform Topology, the terrain is divided into a number of cells, within each cell a node is placed randomly

III. ANALYTICAL MODEL

Our work is based on the following assumptions:

- The MAC protocol is based on a CSMA/CA scheme.

- All the nodes have the same transmission radius R.

- The area of the network can be approximated as a square.

- No mobility is considered.

- The nodes are deployed in either a grid or uniform topology. In a uniform topology, the physical terrain is divided into a number of cells based on the number of nodes in the network, and each node is placed randomly within each cell. Figure 1 shows an example of a uniform topology with 25 nodes in a square area.

The analytical model is described by the following terms:

- Reception Time (T_R): Average time when all the nodes in the network have received the flooded packet.

- Contention Time (T_C): Average time between reception and transmission of a packet by all the nodes in the network.

- Settling Time (T_S): Average time when all the nodes in the network have transmitted the flooded packet and signals the end of the flooding event.

From these definitions we observe that:

$$T_S = T_R + T_C \tag{2}$$

The goal is to minimize the settling time T_S. Since the settling time is the sum of the reception and contention times, the remainder of this section will analyze the relationships between T_R and T_C with respect to the range of the transmission radius.

A. Reception Time

The reception time T_R represents the average time at which nodes received the packet. If the transmission radius of each node is increased, the reception time in the network will decrease; because there are fewer hops needed to reach outlying nodes. The two extreme cases are:

(a) When the nodes have a minimum radius yet the network is still connected.

(b) When the nodes have a radius that covers the entire network.

The first case describes the upper bound of the number of hops required between the source node and the last node to receive the packet. In the second case, all the nodes will be one hop away from the source node, and all of them will receive the packet at approximately the same time, except for negligible differences due to the propagation delay.

Based on the discussion above, the reception time T_R is directly proportional to the maximum distance between any two nodes, and inversely proportional to the transmission radius. Due to the kind of topologies considered in our research (grid or uniform), the maximum distance between the nodes is the diagonal of the network area. Let us define:

R: transmission radius (m).

S: length of the side of the square area (m).

Analytical Reception Time
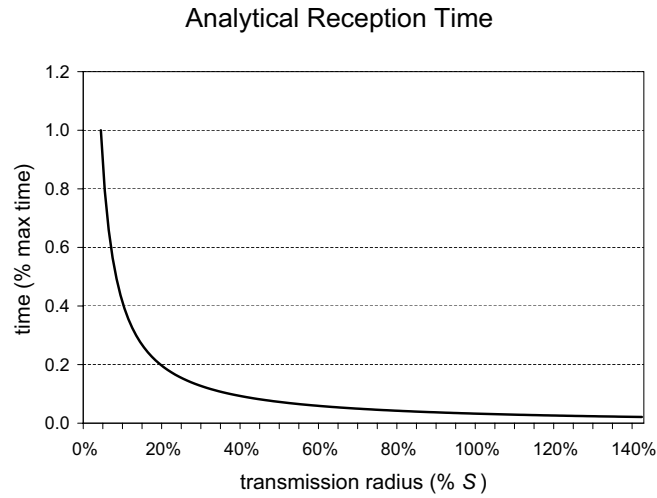
Fig. 2.   Analytical curve for reception time. The X axis represents the range of the transmission radius as a percentage of S (length of the side of the square are). The Y axis represents a normalized time, where 1 is the maximum

Hence, we have the following first-order relationship:

$$T_R = H\frac{S}{R} \tag{3}$$

Where H is a constant.

Figure 2 shows the analytical result for the reception time. It is important to observe that the lower bound of the reception time for any network is equivalent to the transmission delay.

B. Contention Time

Now, let us consider the relationship between the transmission radius and the contention time. If a node increases its transmission radius, it will increase its number of neighbors, which will cause an increase in the contention time.

In order to visualize this effect, we will again consider the two extreme cases analyzed for the reception time .

If the transmission radius is the minimum that guarantees the connectivity of the network, each node will have the minimum number of neighbors possible and thus represents a lower bound of the contention time . On the other hand, when the transmission radius covers the whole network, all the nodes in the network will compete for accessing the medium, thus increasing their contention time.

We observe that the contention time T_C is a function of the number of neighbors. If we consider the area covered by the network as S^2 then the expected number of neighbors of a given node is described by:

$$m = \pi \frac{R^2}{S^2} n \qquad (4)$$

Where n is the total number of nodes in the network.

However, the contention time is not directly proportional to equation 4. There are two phenomena that influence T_C; we name them the *edge phenomenon* and the *back-off phenomenon*. Both of these are described in the following paragraphs.

1) Edge Phenomenon: The edge phenomenon can be described as follows: nodes close to the edges of the network area will not increase their number of neighbors proportionally to the square of the radius. The reason is that only a fraction of the area covered by its transmission radius intersects the area of the network. This phenomenon is illustrated in figure 3, which shows a square topology with a given node placed in the intersection of two lines. In this figure, we can observe three regions as the transmission radius is increased:

- Region 1: When R ranges from 0 to the edge of the network(R_e).
- Region 2: When R ranges from R_e until it covers the entire network (R_w).
- Region 3: When R is greater than R_w.
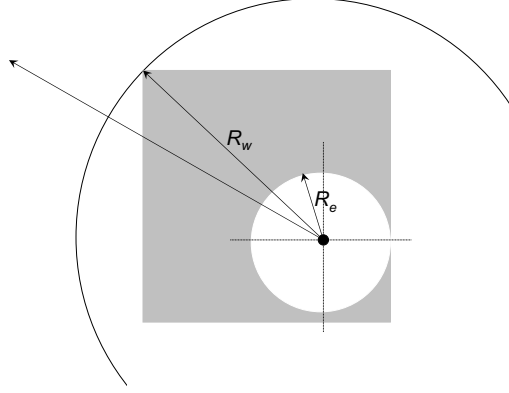
Fig. 3. Different regions to calculate the number of neighbors as we increase the transmission radius of the node. The first region is for values of R between 0 and R_e. The second region goes from R_e to R_w; in this region we can observe that some parts of the coverage area does not contribute with more nodes. In the third region - when R is greater than R_w - all the nodes in the network are neighbors.

Each of these regions will have a different expression for the number of neighbors. For the first region, the number of nodes inside the transmission radius is directly proportional to the square of the radius. In the second region, the number of neighbors increases proportionally to the overlapping area between the transmission range and the network area (please refer to Appendix A). In the third region, the number of neighbors remains constant and is equal to the total number of nodes in the network. Since the values of R for the three different regions depend on the position of the node in the network, we are going to analyze the bounds of the edge phenomenon.

The node closest to the center of the network is the one increasing its number of neighbors most aggressively, hence represents the upper bound. For this node, the second region begins when R is greater than $\frac{S}{2}$ and the third region begins when R is greater than $\frac{S}{2}\sqrt{2}$. The following equation shows the upper bound for the number of neighbors of this node:

$$m, upperbound = \begin{cases} \pi\frac{R^2}{S^2}n & ,0 < R < \frac{S}{2} \\ R^2(\pi - 4\theta + 4cos(\theta)sin(\theta)) & ,\frac{S}{2} < R < \frac{S}{2}\sqrt{2} \\ n & ,\frac{S}{2}\sqrt{2} < R \end{cases} \quad (5)$$
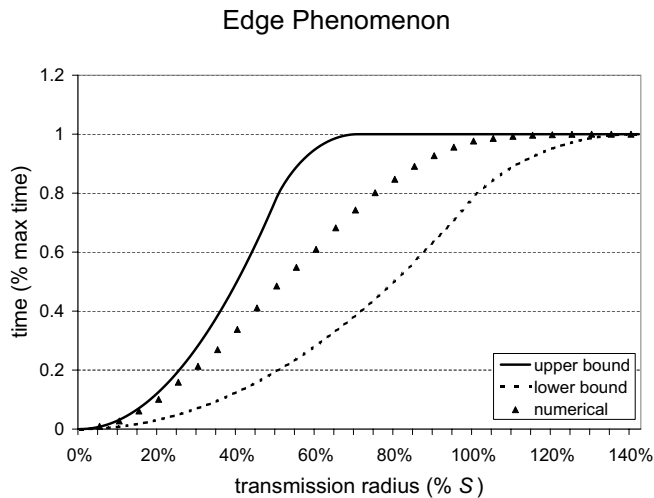
Edge Phenomenon

Fig. 4. Edge phenomenon: the lower and upper bounds are plotted, as well as the curve for the topologies we use.

where

$$\theta = arccos\left(\frac{S}{2R}\right). \tag{6}$$

The lower bound is given by nodes located on the corners of the network. In this case, there is no region 1 as such but rather the number of nodes increases as $\pi\frac{R^2}{4}$ and finishes when R equals S. The second region finishes when R equals $S\sqrt{2}$. The next equation represents the lower bound for the number of neighbors:

$$m, lowerbound = \begin{cases} \pi\frac{R^2}{4S^2}n & , 0 < R < S \\ R^2\left(\frac{\pi}{4} - \phi - cos(\phi)sin(\phi)\right) & , S < R < S\sqrt{2} \\ n & , S\sqrt{2} < R \end{cases} \tag{7}$$

where

$$\phi = arccos\left(\frac{S}{R}\right). \tag{8}$$

Figure 4 shows the curve for the upper and lower bounds of the edge phenomenon. The actual curve of the edge phenomenon, for the kinds of networks we are studying, was obtained through numerical computation, and is also plotted in this figure. As expected, the curve is within the theoretical bounds.

It is important to observe that in some large scale scenarios the transmission radius will not enter regions 2 and 3, due to the large radius R required. However, since we do not have *a priori* knowledge of in what region the optimal radius can be found, we need to take into account all the possible cases in the mathematical model.

2) Back-off Phenomenon: In CSMA/CA protocols, a node checks if the medium is clear before sending a packet; when the medium is clear for a small period of time, the node transmits the packet. If the channel becomes busy during this waiting period, it chooses a random time in the future to transmit the packet. This mechanism leads to a non-linear relationship between the contention time and the number of neighbors. We denote this non-linear relationship as the back-off phenomenon.

Although there are variations in CSMA/CA protocols, usually the back-off timer is calculated by choosing a slot in a contention window and multiplying this number by the slot time. If we denote d_t as the trasnmission delay, n_i as the number of nodes that choose slot i, and b_i as the number of busy slots before slot i, then the contention time is given by:

$$T_C = \frac{\sum_{i=1}^{cw} d_t (1 + b_i) n_i}{n} \tag{9}$$

This equation shows that as the number of nodes increases there is a higher probability that all the slots will be busy; if this the case, if the number of nodes is increased the contention time will reached a maximum value. In practice, this scenario is unlikely because it requires all nodes to be closely synchronized to choose the slot times at almost the same times. A more accurate way to calculate the back-off phenomenon is through simulating a one-hop network with a varying number of nodes. Figure 5 shows the non-linear relationship between the number of neighbors and the contention time. This curve can be numerically approximated by:

$$f(m) = J log^3(m) \tag{10}$$
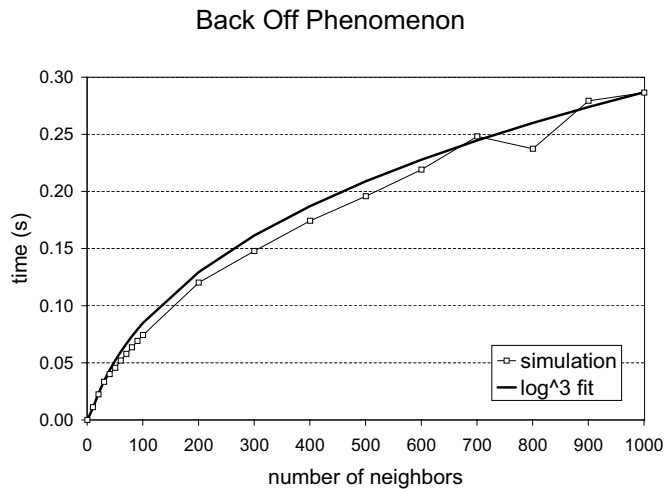
Fig. 5.   Exponential back-off phenomenon: As we can observe, the relation between the contention time and the number of neighbors is not linear

where m is the number of neighbors and J is a constant.

If we incorporate the edge and back-off phenomena explained above, we obtain that the upper bound for the contention time T_C is given by:

$$
T_C, upperbound = \begin{cases} Kf(\pi\frac{R^2}{S^2}n) & ,0 < R < \frac{S}{2} \\ Lf(R^2(\pi - 4\theta + 4cos(\theta)sin(\theta))) & ,\frac{S}{2} < R < \frac{S}{2}\sqrt{2} \\ Mf(n) & ,\frac{S}{2}\sqrt{2} < R \end{cases} \tag{11}
$$

and the lower bound is:

$$
T_C, lowerbound = \begin{cases} Kf(\pi\frac{R^2}{4S^2}n) & ,0 < R < S \\ Lf(R^2(\frac{\pi}{4} - \phi - cos(\phi)sin(\phi))) & ,S < R < S\sqrt{2} \\ Mf(n) & ,S\sqrt{2} < R \end{cases} \tag{12}
$$

Where K, L, and M are constants and $f(.)$ is the function described in equation 10.

Analytical Contention Time
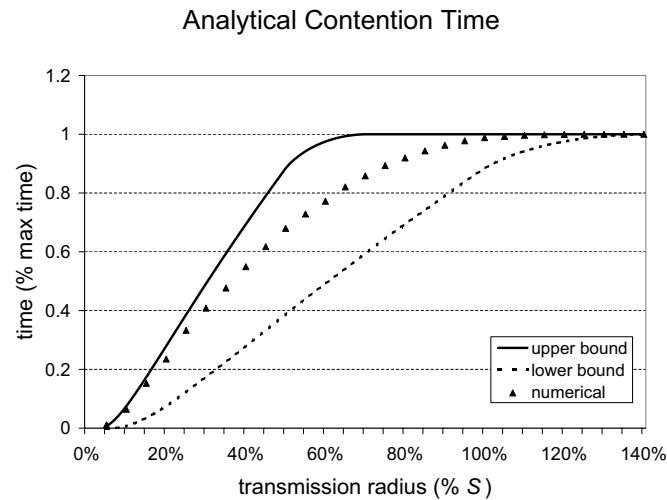
Fig. 6. Analytical curve for the contention time, the upper and lower bounds are plotted as well as the expected curve for a topology of 400 nodes. These curves include the edge and back-off phenomena

Figure 6 shows the respective bounds for the contention time along with the curve obtained through numerical calculations for a network with 400 nodes.

C. Settling Time

Equation 2 stated that the settling time is the sum of the reception and contention times. Figure 7 shows the analytical settling time, again for a network with four hundred nodes. For illustration purposes, the analytical reception and contention times are also plotted. The settling time curve shows a minimum, as expected.

It is important to observe that according to our model, we can obtain improvements up to 60% in the settling time, and the optimal transmission radius is approximately 15% of the length of S. [1]

[1] It is important to observe that as the density decreases the analytical reception time will move towards the right side and will have a smoother fall, implying that the optimal transmission radius will be a higher percentage of S

Analytical Settling Time
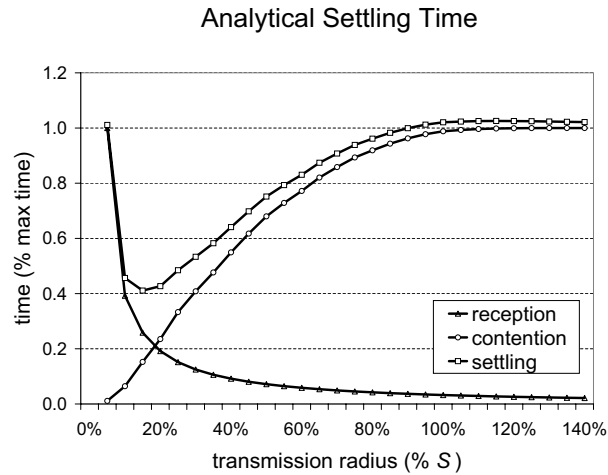
Fig. 7. Analytical curve for the settling time, which is the sum of the reception and contention times

IV. SIMULATION SET UP AND RESULTS

In order to verify our mathematical analysis, we ran a series of simulations and tests. This section describes the set up of the simulations and the results obtained.

A. Simulation Set Up

We simulated different sizes of networks in terms of area and number of nodes. The simulation was done using the Global Mobile Simulation (GloMoSim) developed at UCLA [16]. The MAC layer used for all simulations was CSMA/CA with a bandwidth of 2 Mbps.

First, for each experiment we created a uniform topology placing n nodes in a $S \times S$ square area. All the nodes in the network have the same transmission radius R. Then we determined the minimum radius that connects the network. Starting with that radius, we increased the transmission radius of the nodes until it covered the entire network. The source node, which initiates the flood, is placed at the bottom left corner of the area, hence the maximum transmission radius is set to $R = S\sqrt{2}$. The source sends a packet of fixed size (512 bytes). Usually queries or raw data packets in sensor networks will be smaller than that. We believe that the packet size chosen is

Simulated Settling Time
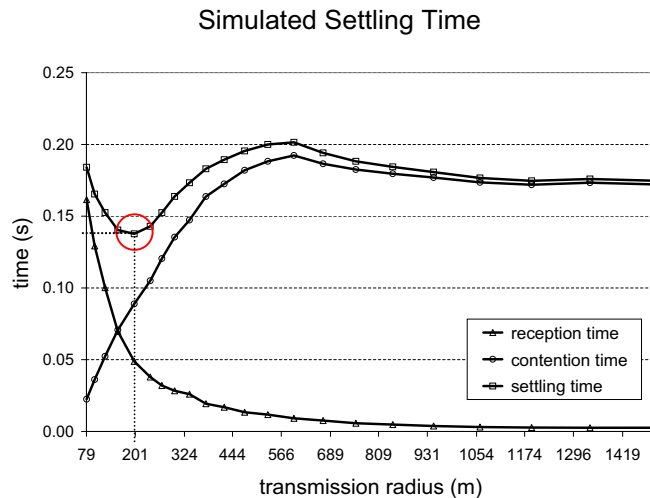
Fig. 8. Reception, contention and settling times obtained through simulations for 400 nodes in a $1000{\times}1000\ m^{2}$ area. Notice that the settling time presents an optimal radius

a reasonable upper bound. Algorithm 1 shows the stages at which we recorded T_R, T_C and T_S.

Algorithm 1: Flooding

if message is received for the first time then

Save receiving time; // used to calculate T_R

Rebroadcast Packet;

Save delivery time; // used to calculate T_C and T_S

B. Results

Figure 8 shows the reception, contention and settling times for 400 nodes in a $1000{\times}1000m^{2}$ area. We observe that the recorded T_R, T_C and T_S resemble their respective analytical counterparts. The settling time shows that an optimal transmission radius can be obtained. In this case, the optimal transmission radius is approximately 200 meters. Table I shows the optimal radius obtained for different topologies. One obvious observation is that as we increase the area of the network – keeping the number of the nodes constant – the optimal transmission radius also increases.

number of nodes	1000 m	2000 m	3000 m	4000 m	5000 m	6000 m	7000 m	8000 m	9000 m	10000 m
225	198.5	335.8	532.2	597.2	843.5	946.7	1191.5	1336.9	1683.0	1888.4
400	198.5	299.3	422.8	597.2	670.0	751.8	843.5	1191.5	1336.9	1500.0
625	157.7	237.7	266.7	376.8	474.3	532.2	670.0	751.8	843.5	946.4
900	157.7	237.7	335.8	376.8	532.2	597.2	597.2	751.8	843.5	1061.9

TABLE I

OPTIMAL RADIUS OBTAINED FOR DIFFERENT TOPOLOGIES IN METERS

number of nodes	1000 m	2000 m	3000 m	4000 m	5000 m	6000 m	7000 m	8000 m	9000 m	10000 m
225	34%	37%	34%	31%	28%	27%	25%	24%	22%	21%
400	32%	36%	33%	29%	27%	24%	23%	20%	20%	18%
625	31%	42%	42%	40%	38%	36%	35%	34%	35%	34%
900	33%	48%	49%	46%	45%	43%	41%	41%	38%	39%

TABLE II

PERCENTAGE OF THE MAXIMUM IMPROVEMENT THAT CAN BE OBTAINED IN THE SETTLING TIME

A metric called the *maximum percentage of improvement* (MPI) is used to quantify the improvement in the settling time obtained by the optimal transmission radius. This metric is defined as:

$$MPI = \frac{\max(T_S) - \min(T_S)}{\max(T_S)} \tag{13}$$

Table II shows that depending on the topology, the maximum percentage of improvement can range up to 50%. The same table also shows that – except for the first two topologies (1000 m and 2000 m) – as we increase the density of nodes, the maximum percentage of improvement also increases. To describe the rationale behind this behavior, we will use figure 9, which shows the reception, contention and settling times for networks with 400, 625, and 900 nodes in a $6000 \times 6000 \ m^2$ area. The first two topologies do not show this trend, due to anomalies that we will explain in the next section.
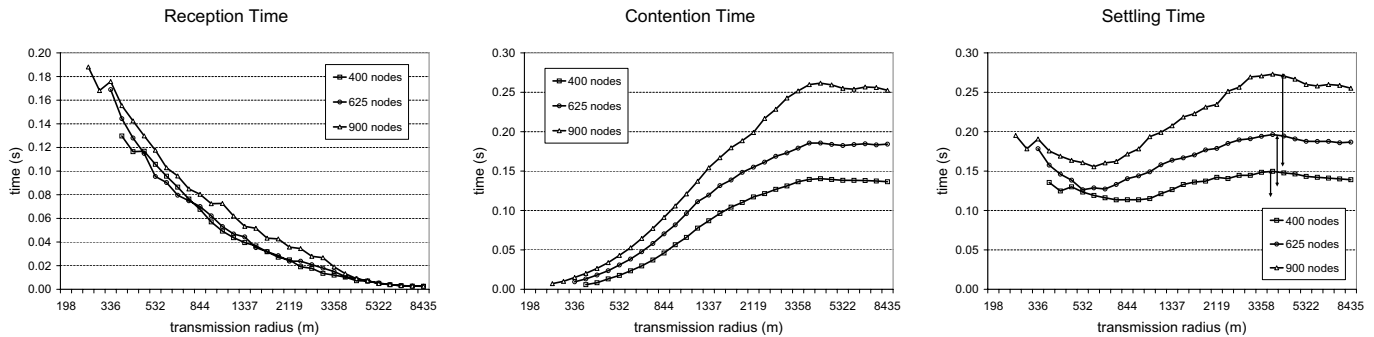
Fig. 9. This figure shows the reception, contention and settling times for networks with 400, 625, and 900 nodes in a $6000 \times 6000 \ m^2$ area. The settling time shows how as the density is increased the maximum percentage of improvement is also increased. This is denoted by the vertical arrows

Figure 9.a illustrates that the reception times follow the same trend [2], and hence are not the cause of the increment in the maximum percentage of improvement. In contrast, figure 9.b depicts clear differences in the contention times. This is due to the fact that – for the same radius – as the density increases, the number of neighbors also increases; and hence the contention time will increase. However, it is important to notice that the differences amongst curves increase as the transmission radius increases. This phenomenon will cause a greater percentage increment in the maximum settling time than in the minimum settling time; which is the reason for the trend observed in Table II. Figure 9.c shows the settling times for the three topologies and it can be clearly observed that the difference between the maximum and minimum settling times increases with the density, as denoted by the vertical arrows.

V. ANOMALIES

The previous section showed that in medium and large areas, an optimal transmission radius is obtained. However, further simulations revealed us that for small areas the optimal transmission radius was not present. As an example, Figure 10 shows the results obtained for 900 nodes in a $200 \times 200 \ m^2$ area. In this case, the settling time does not show an intermediate optimal radius. This section explains the causes of the anomalies and shows that at the root of these is the interference-transmission radius dichotomy which is particularly evident in small areas, depending on the antenna height.

---

[2] The difference in the maximum is because networks with higher densities have a higher number of hops

Absence of Intermediate Optimal
Transigmission Radius
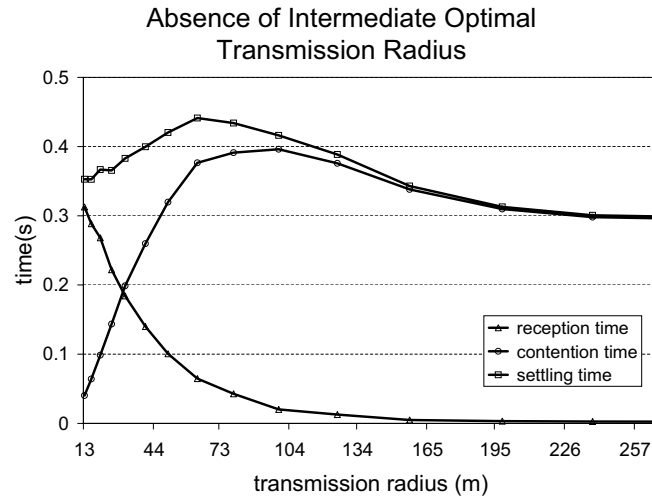
Fig. 10.   This figure shows the reception, contention and settling times for a network with 900 nodes in a $200\times200\ m^2$ area
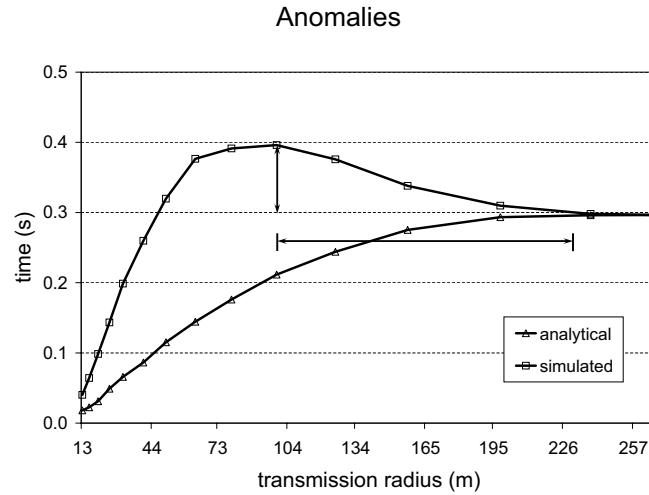
Anomalies

Fig. 11.   Anomalies: The contention time of fig 10 is plotted together with its analytical counterpart. The vertical arrow shows that the maximum contention time is obtained for a smaller transmission radius. The horizontal arrow denotes the non-monotonocity of the contention time

Figure 11 shows the contention time of figure 10, together with the analytical contention time obtained using the model developed in section III. By simple inspection, we observe that the simulated contention time in this case has two major differences with our analytical model. First, the maximum contention time is obtained for a smaller transmission radius than expected (horizontal arrow). Second, after reaching a maximum, the contention time starts to decrease asymptotically to a constant value (vertical arrow). This second effect is counter-intuitive because even if the interference radius causes a maximum contention time earlier, this should at least remain constant, given that

the number of neighbors are either constant or increasing. These two effects together cause the contention time to behave differently than the earlier analytical model, resulting in no intermediate optimal radius for the settling time.

We named the two anomalies mentioned above as: the *early contention phenomenon* and the *non-monotonicity phenomenon*. We will initially give a description of the interference-transmission dichotomy, show exactly how it represents itself in the simulator, and then explain the anomalies in light of this fact.

A. Interference-Transmission Radius Dichotomy

Wireless nodes do not have only a transmission radius but also an interference radius that is greater than the transmission radius. The reception time is mostly dependent on the transmission radius. However, the contention time is dependent on the interference radius. The relationship between interference and transmission radius depends on two factors[3]:

- the propagation model
- the difference between the reception threshold and reception sensitivity of the transceiver.

Two popular radio propagation models used in wireless network simulators are the free-space model and the two-ray model. The two-ray model is a more accurate description of reality, however, it is not accurate for short distances and for these the free-space model is preferred. To overcome this problem, simulators use the free-space model until a specified distance, and beyond this distance the two-ray model is used.

In our case, the reception threshold was ten times greater than the reception sensitivity and the antenna height was 1.5 m. These values mean two things. First, the interference radius is 3.16 times greater than the transmission radius in the free-space model, and 1.78 times greater in the two-ray model. Second, the simulator uses the free-space

[3] These factors are elaborated in Appendix B

Propagation Model in Simulators
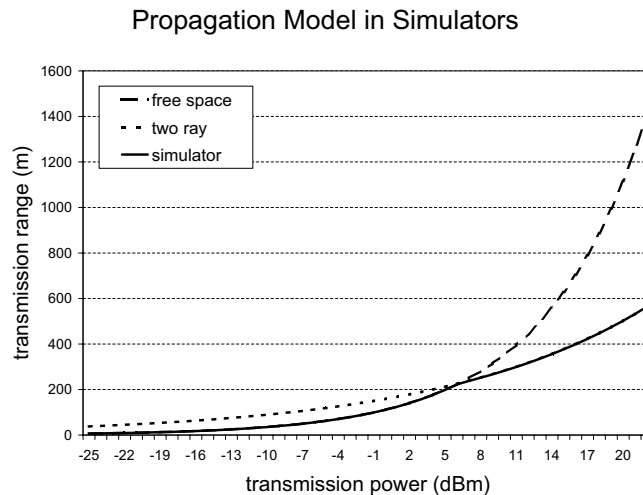
Fig. 12. Propagation Models: the free-space and two-ray model are plotted as dashed lines. The model used by the simulator is the solid line, notice that this *mixed* model uses the free-space model until a transmission radius of 226 m and beyond that uses the two-ray model (the antenna height was 1.5 m)

model for distances smaller than 226.2 meters and beyond this point uses the two-ray model. Figure 12 shows the transmission radius of the free-space and the two-ray model as dotted lines and the model used by the simulators as a solid line. A detailed derivation of the ratios and the intersection point is given in Appendix B.

B. Early Contention Phenomenon in light of the Interference-Transmission Radius Dichotomy

The early contention phenomenon is not only observed in the topology showed in figure 10. A closer look to the simulation results obtained in section IV (figure 8) shows that the maximum contention time is appearing for a transmission radius of 600 m. However, the derived analytical model in figure 6 showed that this maximum should be obtained for a transmission radius of approximately 1000 m[4].

As we have explained in the previous paragraphs, the contention time is not solely dependent on the transmission radius but better described as dependent on the interference radius. Because the interference radius covers a larger area than the transmission radius, it is not surprising to see a maximum contention at a smaller transmission radius.

[4] 1000 m is obtained because the analytical model of figure 6 shows that the maximum contention time for a network with 400 nodes is reached when the transmission radius is equal to 100% S, which is 1000 m in this case
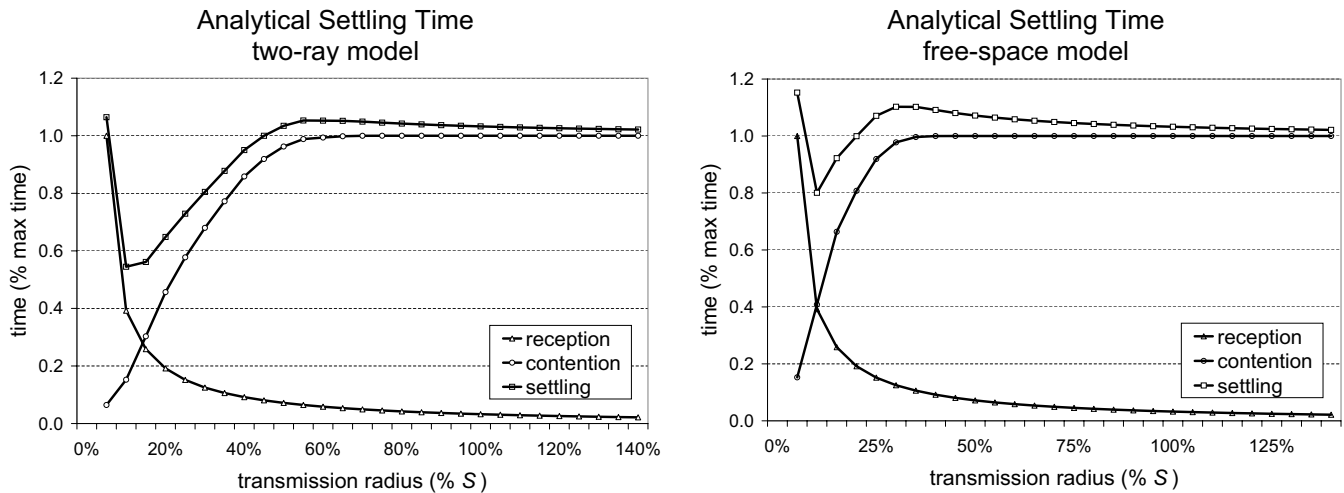
Fig. 13. These figures shows the analytical curves taking into account interference in the two-ray and free-space propagation models. It is important to observe that the minimum settling time is greater than the first model (fig 7)

Figure 13 shows how the contention time (and settling time) is shifted by including the interference-transmission radius ratio in the analytical model. Important observations for the new model are that the improvement obtained by the optimal transmission radius is reduced and that the maximum contention time now is reached when the interference radius covers the entire network. This new model better describes the simulations obtained.

C. Non-Monotonicity Phenomenon in light of the Interference-Transmission Radius Dichotomy

The non-monotonicity phenomena is particularly obvious for higher interference-transmission radius ratios. We found that this phenomena occurs due to MAC layer synchronization effects that depend on whether interfering nodes are within interference/transmission range of each other. It is best illustrated with an example. Figure 14 shows two scenarios. In the upper one the transmission radius is to the left of the maximum contention time, while in the lower one is to the right. In the first scenario, nodes A and C are waiting to transmit their packets. At time t_1 node B's back-off timer expires and starts transmitting the packet, node A is within node B's interference range and hence freezes its timer, however node C is outside this range and continues to decrease its timer. At time t_2 node C's timer also expires and starts transmitting its packet, finishing its transmission at time t_4. Node A will have to wait the interval between t_1 to t_4 due to the transmissions of these two nodes. In the second scenario,
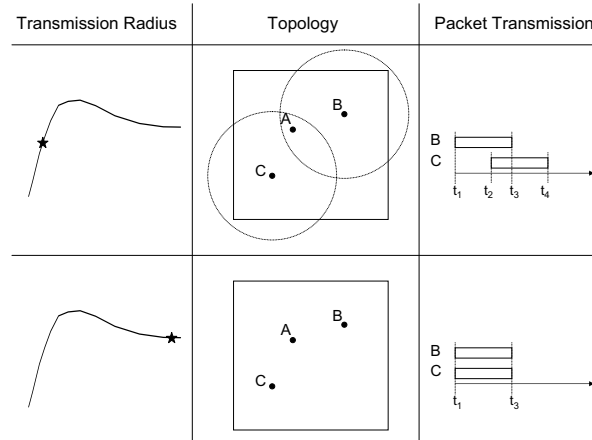
Fig. 14. Non-Monotonicity phenomenon: after reaching a maximum, the contention time starts to decrease asymptotically to a constant value. This figure shows the importance that synchronization has on this phenomenon. The star in the contention time curve shows the transmission radius that is being analyzed

all the nodes received the flooded packet at almost the same time and upon reception choose an slot time of their contention window. Let us assume that nodes B and C choose the same slot s_i and node A choose slot s_j, which is greater than s_i. In this scenario, nodes B and C will sense that the channel is idle at the same time and will start transmitting their packets at t_1 and finish their transmissions at t_3. In this case node A will have to wait only during the interval t_1 to t_3.

The key difference between the two scenarios described above is synchronization. When the transmission radius covers the entire network, the network will resemble a single slotted-Aloha access channel, where all the nodes choosing the same slot will collide with high probability. Because of this, for every node that waits (stops its timer) because it observes a collision, there is a good probability that several transmission are overlapping with each other, and therefore that node has to wait for a smaller contention time. On the other hand, when the interference radius starts to cover the whole network the nodes will be highly de-synchronized and hence every time a node stops it will be interrupted for a longer amount of time because the nodes' transmissions do not overlap too much with each other.

It is important to remark that after reaching the maximum contention time, the transmission radius starts to cover

more area of the network while the interference range looses its area of coverage. This implies that more nodes are synchronized, and that, is the reason why we have the decay in the contention time.

Thus, paradoxically, we find that *increasing the transmission radius (beyond the point where the interference radius covers the network) does not increase the amount of contention but rather decreases the contention time for nodes waiting to transmit, because the contending transmissions become more synchronized and more likely to use perfectly overlapping times*.

To summarize this discussion, we find that the early-contention and non-monotonicity phenomena are anomalies that can cause the absence of an optimal intermediate transmission radius that minimizes the settling time. However, these anomalies (which have to do with the dichotomy between the transmission and interference radius) are most noticeable in small areas (< 200m) when antenna heights are significant (~ 1.5m).

VI. CONCLUSIONS AND FUTURE WORK

This paper addresses the problem of finding an optimal transmission radius for minimizing the settling time for flooding in sensor networks. This problem merits discussion because flooding is still used in various wireless protocols, and this paper proposes a new way to adjust the transmission radius to make this task more efficient.

There is significant amount of work in the literature that has studied the optimal transmission radius for maintaining network connectivity and making efficient use of energy in the network. However, finding an optimal transmission radius to minimize the settling time in flooding events has not been addressed in depth before.

This work proves that choosing a transmission radius without previous analysis can lead to an unnecessarily large settling time in the network which will decrease the overall network throughput. We proposed an analytical model verified by simulations that describes an optimal transmission radius for uniform and grid topologies.

We also found that some scenarios do not demonstrate an intermediate optimum transmission radius. We analyzed

these effects in terms of the early contention and non-monotonicity phenomena, which were shown to be due to the interference-transmission radius dichotomy.

Thus, the important contributions of this work are the:

- Development of a mathematical model investigating the tradeoff between contention and reception times for flooding in large scale wireless sensor networks.

- Analysis of optimal transmission radius that minimizes the settling time.

- Demonstration through simulations that improvements up to 50% can be achieved in the settling time, particularly for dense deployments in large areas.

- Investigation of anomalies relating to the interference-transmission dichotomy and and their influence on the settling time behavior of flooding.

To our knowledge there are few results in the literature that analyze the behavior of network layer protocols for large-scale wireless systems while taking into account the underlying MAC-layer behavior. In this paper we have focused on analyzing the impact of medium access on what is perhaps the simplest wireless information dissemination protocol - basic broadcast flooding. We hope to continue this line of work by investigating the joint behavior of other protocols for wireless networks with respect to the underlying MAC layer.

REFERENCES

[1] Akyildiz, I.F., Su, W., Sankarasubramaniam, Y., and Cayirci, E., "A Survey on Sensor Networks, IEEE Communications Magazine," Vol. 40, No. 8, pp. 102-116, August 2002.

[2] Chalermek Intanagonwiwat, Ramesh Govindan and Deborah Estrin, "Directed diffusion: A scalable and robust communication paradigm for sensor networks" In Proceedings of the Sixth Annual International Conference on Mobile Computing and Networking (MobiCOM '00), August 2000.

[3] S. Ni, Y. Tseng, Y. Chen, and J. Chen, "The broadcast storm problem in a mobile ad hoc network," In Annual ACM/IEEE International Conference on Mobile Computing and Networking (MOBICOM), pp. 151-162, August 1999.

[4] Deepak Ganesan, Bhaskar Krishnamachari, Alec Woo, David Culler, Deborah Estrin and Stephen Wicker, "Complex Behavior at Scale: An Experimental Study of Low-Power Wireless Sensor Networks", UCLA Computer Science Technical Report UCLA/CSD-TR 02-0013

[5] P. Gupta and P. R. Kumar, "Critical Power for Asymptotic Connectivity in Wireless Networks," in Stochastic Analysis, Control, Optimization and Applications, Eds.W.M.McEneany et al., Birkhauser, Boston, p. 547-566, 1998.

[6] Feng Xue and P. R. Kumar, "The number of neighbors needed for connectivity of wireless networks." Submitted to Wireless Networks. April 1, 2002.

[7] L. Kleinrock and J . A. Silvester. "Optimum transmission radii for packet radio networks or why six is a magic number" in Conf. Rec. Nat. Telecommun. Conf., Dec. 1978, pp. 4.3.1-4.3.5.

[8] M. Sanchez , P. Manzoni and Z. J. Haas, "Determination of Critical Transmission Range in Ad-Hoc Networks," Multiaccess Mobility and Teletraffic for Wireless Communications Workshop (MMT99), Venice, Italy, October 1999.

[9] TinyOS Homepage. http://webs.cs.berkeley.edu/tos/

[10] Takagi, H. and L. Kleinrock, "Optimal Transmission Ranges for Randomly Distributed Packet Radio Terminals", IEEE Transactions on Communications, Vol. COM-32, No. 3, pp. 246-257, March 1984.

[11] Bhaskar Krishnamachari and Stephen B. Wicker, "Critical Transmission Range for Channel Allocation in Multi-hop Wireless Networks" in submission, July 2002.

[12] David Braginsky and Deborah Estrin, "Rumor Routing Algorithm For Sensor Networks" First Workshop on Sensor Networks and Applications (WSNA), September 28 2002, Atlanta, GA.

[13] K. Sohrabi, J. Gao, V. Ailawadhi, G.J. Pottie. "Protocols for self-organization of a wireless sensor network" IEEE Personal Communications, vol.7, no.5, pp 16-27, Oct 2000

[14] Alec Woo, David Culler. "A Transmission Control Scheme for Media Access in Sensor Networks" Mobicom 2001

[15] An Energy-Efficient MAC Protocol for Wireless Sensor Networks Wei Ye, John Heidemann and Deborah Estrin In Proceedings of the 21st International Annual Joint Conference of the IEEE Computer and Communications Societies (INFOCOM 2002), New York, NY, USA, June, 2002.

[16] Global Mobile Information Systems Simulation Library http://pcl.cs.ucla.edu/projects/glomosim/

[17] H.T. Friis. A note on a simple transmission formula. Proc. IRE, 34, 1946.

[18] T.S. Rappaport. Wireless Communications, principles and practice. Prentice Hall, 1996.

[19] Marco Zuniga Z. and Bhaskar Krishnamachari. "Optimal Transmission Radius for Flooding in Large Scale Wireless Sensor Networks" Interbational Workshop on Mobile and Wireless Networks, Providence, RH, USA, May, 2003

[20] E.M. Royer, P.M. Melliar-Smith, and L.E. Moser. "An analysis of the optimum node density for ad hoc mobile networks" In Proc. International Conference on Communications, 2001.

[21] L. Li, V. Bahl, Y.M. Wang, and R. Wattenhofer. "Distributed topology control for power efficient operation in Multihop Wireless Ad-Hoc Networks" In Proc. IEEE INFOCOM '01, April 2001.

[22] Li Xiao, Zhichen Xu. "On Energy Efficiency and Network Connectivity of Mobile Ad Hoc Networks". In Proc. of ICDCS '03, Providence, RH, USA, May, 2003

VII. APPENDIX A : OVERLAPPING OF TRANSMISSION RADIUS AND NETWORK AREAS

We are interested in obtaining the overlapping area (A_o) as shown in figure 15. Defining A_r as the residual area beyond $S/2$, because of symmetry, the total overlapping area is given by:

$$A_o = 8\left(\frac{\pi R^2}{8} - A_r\right) \tag{14}$$

where

$$A_\theta = A_r + A_t \tag{15}$$

It is observed that

$$\theta = arccos\left(\frac{S}{2R}\right) \tag{16}$$

Hence

$$A_\theta = \theta \frac{R^2}{2} \tag{17}$$

and

$$A_t = R^2 sin(\theta) cos(\theta) \tag{18}$$

as a consequence

$$A_r = \theta \frac{R^2}{2} - R^2 sin(\theta) cos(\theta) \tag{19}$$

Finally we obtain

$$A_o, center = 8\left(\frac{\pi R^2}{8} - \theta \frac{R^2}{2} - R^2 sin(\theta) cos(\theta)\right)$$
$$A_o, center = R^2 (\pi - 4\theta - 4sin(\theta) cos(\theta)) \tag{20}$$

In the case of the lower bound, we have one fourth of a circle and ϕ is given by:

$$\phi = arccos\left(\frac{S}{R}\right). \tag{21}$$
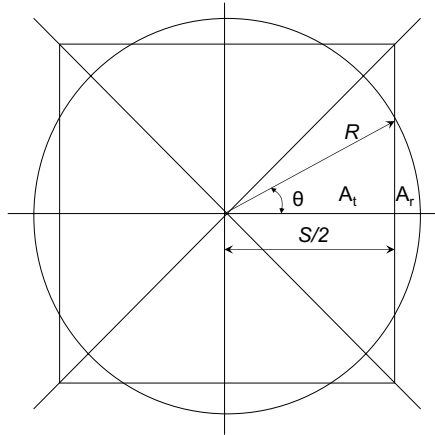
Fig. 15. The figure shows the overlapping area between the transmission radius coverage and the area of the network

Hence:

$$A_o, corner = 2\left(\frac{\pi R^2}{8} - \phi\frac{R^2}{2} - R^2 sin(\phi)cos(\phi)\right)$$

$$A_o, corner = R^2\left(\frac{\pi}{4} - \phi - sin(\phi)cos(\phi)\right)$$

(22)

VIII. APPENDIX B : PROPAGATION MODELS AND INTERFERENCE VERSUS TRANSMISSION RADIUS

The relation between the transmission and interference radius is related to the propagation model of the transmission medium. We are going to briefly describe two of the most common models, the free-space model and the two-ray model.

The *free-space* propagation model assumes the ideal condition where there is only one line-of-sight path between transmitter and receiver. [17] presents the following equation to calculate the signal power at a distance d from the transmitter:

$$Pr(d) = \frac{P_t G_t G_r \lambda^2}{(4\pi)^2 d^2 L}$$

(23)

Where P_t is the transmitter signal power, G_t and G_r are the antenna gains of the transmitter and receiver respectively,

L ($L < 1$) is the system loss and λ is the wavelength.

The *two-ray* model [18] considers a direct path and a ground reflection path, and is more accurate for long distances than the free-space model. In this model the received power at distance d is given by:

$$Pr(d) \;=\; \frac{P_t G_t G_r h_t^2 h_r^2}{d^4 L} \tag{24}$$

Now, let us obtain the relation between the transmission and interference range. A transceiver has two important parameters:

Power Reception Threshold (P_h): minimum power for received packet.

Power Reception Sensitivity (P_s): sensitivity of the radio.

Where $P_h > P_s$. If a node receives a signal above P_h it process the packet, this determines the transmission radius. If a node receives a signal above P_s but below P_h, it senses the channel as busy but is unable to process the packet, this determines the interference range.

Given that a transmitter sends a signal with power P_t, let us define the transmission radius R_t as the distance a signal travels until the power decays to P_h and the interference radius R_s as the distance a signal travels until decays to P_s.

Some basic mathematical manipulation will give:

$$\frac{R_t}{R_s} \;=\; \sqrt{\frac{P_s}{P_h}} \tag{25}$$

for the free-space model, and:

$$\frac{R_t}{R_s} \;=\; \sqrt[4]{\frac{P_s}{P_h}} \tag{26}$$

For the two-ray model. Another important feature of the propagation models is that if the two-ray model is selected then it has to be calculated the minimum distance until it is valid. As figure 12 shows there is an intersection point below which the free-space model has to be used. The distance at which both intersect is given by:

$$d_i \;=\; \frac{4\pi h_t h_r}{\lambda} \tag{27}$$